CRACK GROWTH UNDER INTERMITTENT OVERLOADS

L. P. Borrego[1], J. M. Costa[2] and J. M. Ferreira[2]

[1]Department of Mechanical Engineering, Instituto Superior de Engenharia de Coimbra - ISEC, Rua Pedro Nunes, Quinta da Nora, 3030-199 Coimbra, Portugal
[2] Department of Mechanical Engineering, University of Coimbra, Polo II, Pinhal de Marrocos, 3030-201 Coimbra, Portugal

Abstract. This study analyses the fatigue crack growth behaviour in AlMgSi1-T6 aluminium alloy due to several loading sequences containing intermittent overloads. The fatigue crack propagation tests have been performed in load control mode using Middle-Tension specimens. Two stress ratios: R=0.05 and R=0.4, and four intermediate baseline cycles: n_{BL}=10, n_{BL}=100, n_{BL}=1000 and n_{BL}=10000, were analysed. Crack closure was monitored in all tests by the compliance technique using a pin microgauge. The observed fatigue crack growth behaviour is compared to constant amplitude loading and discussed in terms of the intermediate baseline cycles and stress ratio. The crack closure parameter *U* was obtained and compared with the crack growth transients. For less frequently applied overloads crack retardation was observed, while the results for 10 baseline cycles between overloads presented crack acceleration. In spite of some discrepancy, attributed to the quick change of the closure levels, it is clear that plasticity-induced crack closure plays an important role on the load interaction effects observed in this aluminium alloy.

Resumo. Este estudo analisa o comportamento de propagação de fendas por fadiga na liga de alumínio AlMgSi1-T6 provocado por diversas sequências de carga contento sobrecargas periódicas. Os ensaios de propagação de fenda foram realizados em controlo de carga utilizando provetes Middle-Tension. Foram analisados duas razões de tensão: R=0.05 e R=0.4, e quatro espaçamentos entre sobrecargas: n_{BL}=10, n_{BL}=100, n_{BL}=1000 and n_{BL}=10000. O comportamento do crescimento da fenda obtido é comparado com o verificado em amplitude de carga constante e discutido em termos da periodicidade de aplicação das sobrecargas e da razão de tensão. O parâmetro normalizado da razão de carga *U* foi determinado e comparado com o comportamento transitório da velocidade de propagação. Para as sobrecargas aplicadas com menos frequência foi observado o retardamento do crescimento da fenda, enquanto que os resultados para sequências de carga com 10 ciclos intermédios entre sobrecargas mostraram aceleração da fenda. Apesar de alguma discrepância, atribuída á rápida variação do nível de fecho de fenda, é claro que o fecho de fenda induzido por plasticidade desempenha um papel importante nos efeitos de interacção de carga observados nesta liga de alumínio.

1. INTRODUCTION

It is widely known that in the last decade's aluminium alloys have been more and more used in the production industry, mainly in ground transport systems. The 6xxx series alloys are commonly use in structural applications due to the fact of presenting relatively high strength, good corrosion resistance and high toughness combined with good formability and weldability.

For many fatigue critical parts of structures, vehicles and machines, fatigue crack propagation under service conditions generally involves random or variable amplitude, rather than constant amplitude loading conditions. When a fatigue crack is subjected to these load variations accelerations and/or retardations in crack growth rate can occur. Thus, an accurate prediction of fatigue life requires an adequate evaluation of these load interaction effects.

The majority of the work carried out in this field has been on the effects of single peak tensile overloads [1-4] simply because this type of loading can lead to significant load interaction effects. In contrast, other variable amplitude load sequences have not yet been exhaustively investigated. Among them, intermittent or periodic overloads [5, 6] are experienced by a large number of engineering components.

Several mechanisms have been proposed to explain crack growth retardation following single peak tensile overloads, which include models based on residual stress, crack closure, crack tip blunting, strain hardening, crack branching and reversed yielding. However, the precise micromechanisms responsible for the load interaction effects are not fully understood.

In recent work the authors concluded that the plasticity-induced crack closure argument could generally explain the crack growth behaviour following single peak

[1] Corresponding author: e-mail borrego@isec.pt, Tel +351239790330

overloads [3, 4]. The present work intends to analyse the fatigue crack growth due to several loading sequences containing periodic overloads and to clarify if the observed behaviour can also be correlated with the crack closure phenomenon.

2. EXPERIMENTAL DETAILS

This research was conduced using the AlMgSi1 (6082) aluminium alloy with a T6 heat treatment. The T6 heat treatment corresponds to a conversion of heat-treatable material to the age-hardened condition by solution treatment, quenching and artificial age-hardening. The chemical composition and the mechanical properties of the alloy are shown in tables 1 and 2, respectively.

Table 1. Chemical composition of the AlMgSi1-T6 aluminium alloy [% Weight].

Si (%)	Mg (%)	Mn (%)	Fe (%)	Cr (%)
1.05	0.80	0.68	0.26	0.01

Table 2. Mechanical properties of the AlMgSi1-T6 aluminium alloy.

Tensile strength, σ_{UTS} [MPa]	300±2.5
Yield strength, σ_{YS} [MPa]	245±2.7
Elongation, ε_r [%]	9
Cyclic hardening exponent, n'	0.064
Cyclic hardening coefficient, K' [MPa]	443
Fatigue strength exponent, b	-0.0695
Fatigue strength coefficient, σ'_f [MPa]	485
Fatigue ductility exponent, c	-0.827
Fatigue ductility coefficient, ε'_f	0.773

The fatigue tests were conducted using (MT) specimens with a thickness of 3 mm, in agreement with the ASTM E647 standard [7]. The specimens were obtained in the longitudinal transverse (LT) direction from a laminated plate. Fig. 1 illustrates the major dimensions of the samples used in the tests. The notch preparation was made by electrical-discharge machining. After that, the specimens surfaces were polished mechanically.
All experiments were performed in a servohydraulic, closed-loop mechanical test machine with 100 kN load capacity, interfaced to a computer for machine control and data acquisition. All tests were conducted in air, at room temperature and with a frequency of 20 Hz. The specimens were clamped by hydraulic grips. The crack length was measured using the d.c. potential drop method. Collection of data was initiated after achieving an initial crack length $2a_0$ of approximately 12 mm.

The influence of intermittent overloads was investigated in the Paris regime at R=0.05 and R=0.25. The tests were performed under load control mode. Periodic overloading was started after the crack had grew to a crack length corresponding to ΔK=6 MPa $m^{1/2}$. The overload ratio OLR was kept constant at 1.5 which was defined as:

$$OLR = \frac{\Delta K_{OL}}{\Delta K_{BL}} = \frac{K_{OL} - K_{min}}{K_{max} - K_{min}} \quad (1)$$

where K_{max}, K_{min}, and K_{OL} are the maximum, minimum and peak overload intensity factors, respectively. Therefore, each overload was applied with 50% increase in load respectively to the baseline loading range. The overloads were applied during one cycle, each 10, 100, 1 000 and 10 000 baseline cycles by previously programming the respective entire load sequence. The crack growth rates were determined by the secant method [7].

Load-displacement behaviour was monitored at specific intervals using a pin microgauge. The gauge pins were placed in the two drilled holes of 0.5 mm diameter located above and below the centre of the notch (Fig. 1). The distance between these holes was 3.5 mm. In order to collect as many load-displacement data points as possible during a particular cycle, the frequency was reduced to 0.5 Hz.

From the load-displacement records, variations of the opening load P_{op}, were derived using the technique known as maximisation of the correlation coefficient. This technique involves taking the upper 10% of the P-ε data and calculating the least squares correlation coefficient. The next data pair is then added and the correlation coefficient is again computed. This procedure is repeated for the whole data set. The point

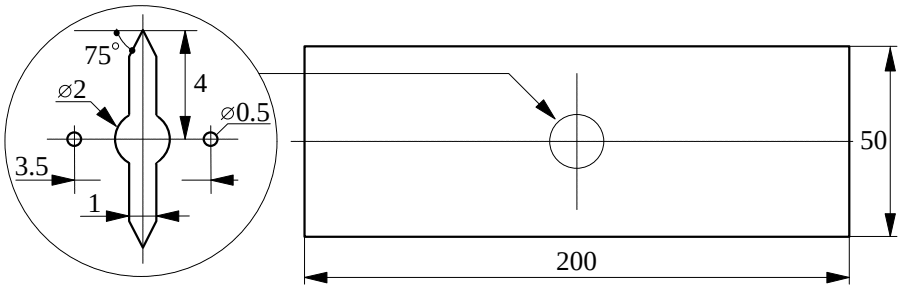

Fig. 1. Geometry of the M(T) specimen used in this work (dimensions in mm).

at which the correlation coefficient reaches a maximum could then be defined as P_{op}.

The fraction of the load cycle for which the crack remains fully open, parameter *U*, was calculated by the following equation:

$$U = \frac{P_{max} - P_{op}}{P_{max} - P_{min}} \quad (2)$$

The values of the effective stress intensity factor range, ΔK_{eff}, are given by the expression:

$$\Delta K_{eff} = K_{max} - K_{op} = U\Delta K \quad (3)$$

During all the tests, the crack path at the specimen surface was carefully observed using an optical microscope. The fracture surfaces were observed in a Philips XL30 scanning electron microscope.

3. RESULTS AND DISCUSSION

3.1. Typical transient behaviour and periodicity effect

The effect of periodically applied overloads for several numbers of baseline cycles between overloads, n_{BL}, can be seen in Fig. 2. In Fig. 2(a), the crack length is plotted against the number of cycles, and Fig. 2(b) presents the correspondent crack growth response as a function of ΔK. The behaviours under constant amplitude loading and for a single peak overload are superimposed for comparison.

For remotely spaced overloads (n_{BL} 100 cycles) crack retardation and a corresponding decrease of *da/dN* relatively to constant amplitude loading are observed. As depicted in Fig. 2(a) the crack only reaches 10 mm length after more 80%, 200% and 300% for respectively, 100, 1 000 and 10 000 intermediate baseline cycles, than those elapsed under constant amplitude loading to achieve the same crack length. Therefore, the longer the spacing n_{BL} between overloads the more severe retardation is produced. Moreover, the retardation of crack growth is always greater for periodic overloads applied with n_{BL} 100 cycles than for the equivalent single peak overload. It is important to notice that maximum retardation occurred when tensile overloads were applied at a periodicity which was near the number of cycles associated to the minimum *da/dN* value attained for the single overload (11 600 cycles).

In contrast, the results for more frequently applied overloads (n_{BL}=10 cycles) present crack acceleration relatively to constant amplitude loading. For this loading condition, the crack length reached 10 mm after less 25 402 cycles than under constant amplitude loading, representing a fatigue life decrease of approximately 20%.

An interesting feature that can be seen in Fig. 2(b) is that after application of the first overload the crack growth rate exhibits three distinct stages. Initially, a retardation period identical to that induced by a single peak overload is observed for less frequently applied overloads. For overloads applied each 10 baseline cycles this initial stage is similar to the one generally observed after an underload. The subsequent crack growth rate increases in a stable manner. Finally, for *DK* values above approximately 10.5 MPa $m^{1/2}$ the crack growth rate increases more rapidly.

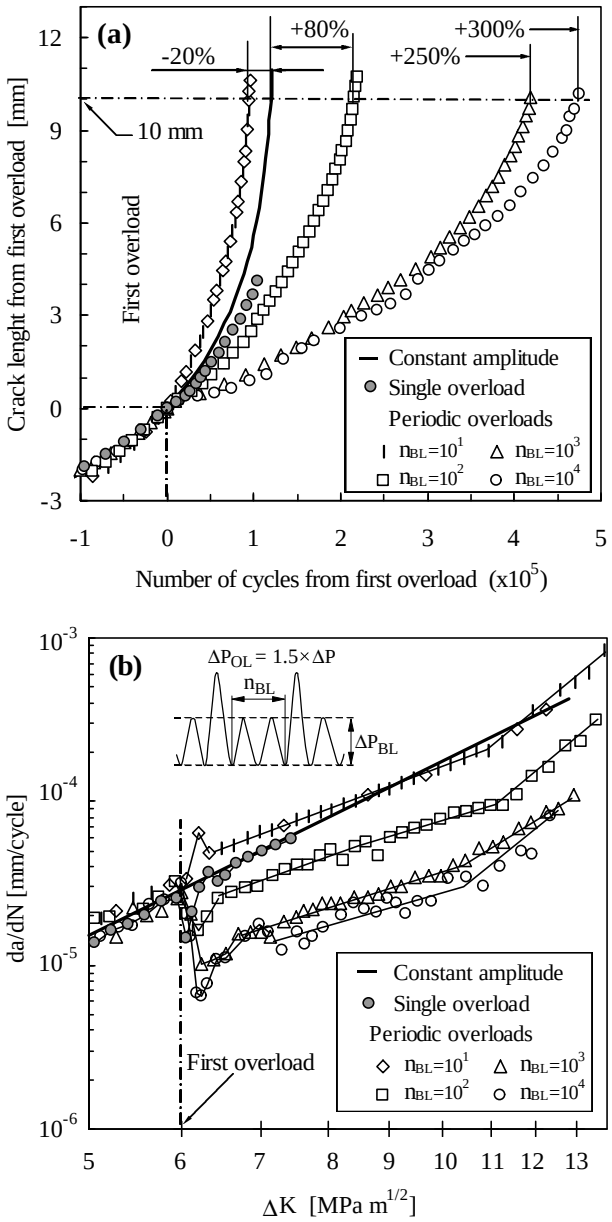

Fig. 2. Effect of the spacing between overloads, R=0.05: (a) a versus N; (b) da/dN versus ΔK.

During the crack growth rate decrease, the minimum crack growth rate value was attained only after approximately 29 000, 38 000 and 55 000 cycles for n_{BL}=100, n_{BL}=1 000 and n_{BL}=10 000, respectively. Furthermore, the initial retardation period persisted for

several thousand cycles, approximately 52 000, 112 000 and 125 000 cycles for 100, 1 000 and 10 000 intermediate baseline cycles, respectively. These values are significantly higher then those due to an equivalent single overload, respectively, 11600 and 33 700 cycles, indicating a strong interaction between overloads in the beginning of there application. This interaction will induce progressively lower transient crack growth rates as indeed observed.

The initial retardation period persisted during approximately 1 mm for all the less frequently applied overloads (n_{BL} 100 cycles), which curiously equals the single overload affected crack length (0.99 mm). This stage includes the minimum crack growth rate which was achieved at approximately 0.35 mm for all n_{BL} 100 cycles. This crack increment represents approximately 1/3 of the equivalent single overload affected crack length.

It becomes obvious from Fig. 2(b) that during the stable crack growth rate stage the retardation in crack growth rate increases with ΔK for n_{BL} 100 cycles. For overloads applied with 10 intermediate baseline cycles the acceleration in crack growth rate decreases with ΔK and for ΔK values above 10 MPa $m^{1/2}$ even some crack growth retardation is observed. Similar experimental results were reported in [6]. This is not surprising because the monotonic plastic zone produced by the overloads increases with ΔK.

3.2. Stress ratio effect

The effect of intermittent overloads at R=0.4 for 100 and 1 000 baseline cycles are shown in Fig. 3. The corresponding results obtained for intermittent overloads at R=0.05 and under constant amplitude loading are also superimposed.

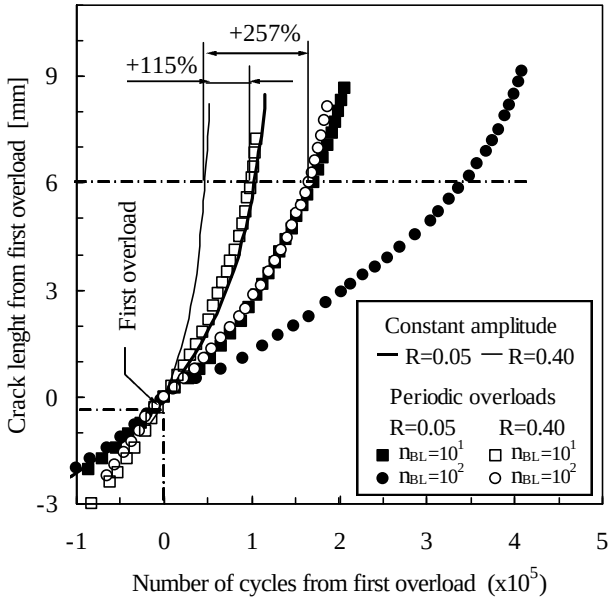

Fig. 3. Influence of stress ratio.

This figure shows that the crack retardation effect is lower at higher mean stress. For example, in order to the crack attain 6 mm are needed more 53 496 and 119 039 cycles for 100 and 1 000 intermediate baseline cycles, respectively, than those elapsed under constant amplitude loading at R=0.4. It is important to notice than these number of cycles are lower then those obtained at R=0.05 to reach the same crack length (67 032 for n_{BL}=100 and 245 127 for n_{BL}=1 000). However, at R=0.4 they correspond to a larger relative increment of crack growth: 115% and 257% for n_{BL}=100 and n_{BL}=1 000, respectively.

3.3. Crack closure

The measured crack closure levels at R=0.05 are exhibited in Fig. 4. The obtained data are plotted in terms of the normalized load ratio parameter, *U*, calculated by eq. (2), against *DK*. The acquisition of each load-displacement record was carried out approximately at half interval between successive overloads. Therefore, the depicted *U* values have to be understood as corresponding to mean closure levels.

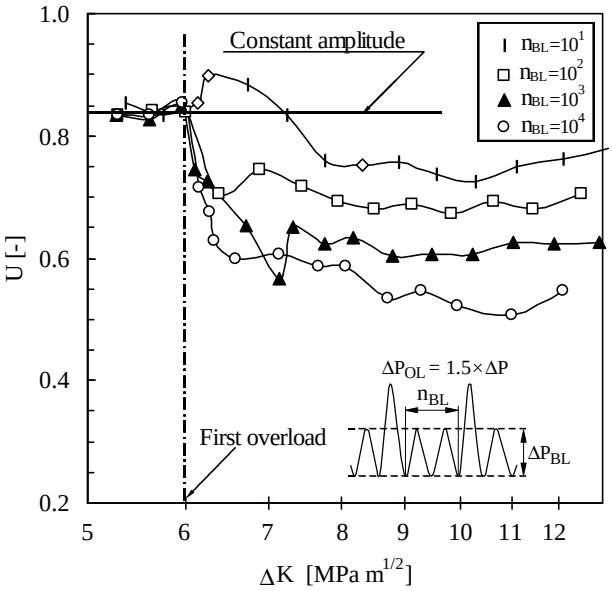

Fig. 4. Mean closure levels for periodic overloads, R=0.05.

It becomes evident that the crack closure data show basically the same trend as the corresponding experimentally observed crack growth rate response. Moreover, the influence of n_{BL} is in agreement with the different closure levels. Fig. 4 shows that, except during a small range of *DK* following the first overload for n_{BL}=10, the crack closure level for periodically applied overloads is significantly higher than for constant amplitude loading. Furthermore, the crack closure level increases (*U* decreases) with the number of intermediate baseline cycles.

Prior to the first overload the *U* parameter at the baseline loading level is relatively stable. Upon

application of the first overload the crack closure level increases quickly for remotely spaced overloads and decreases for closely spaced overloads, followed by a slow increase or even certain stabilization. There is also a small decrease of the crack closure level at *DK* values above approximately 10 MPa $m^{1/2}$. The minimum value of *U* attained was 0.73, 0.67, 0.57 and 0.51 for 10, 100, 1 000 and 10 000 intermediate baseline cycles, respectively, corresponding to a decrease of approximately 13%, 20%, 32% and 39% relatively to the *U* baseline level in constant amplitude loading. The crack closure levels measured at 1 000 and 10 000 intermediated baseline cycles are closely to each other as also observed for the corresponding crack growth rates (see Fig. 2).

The crack closure level measured for closely spaced overloads (n_{BL}=10) is higher then for the baseline loading only in the *DK* range between 6 and 7 MPa $m^{1/2}$. However, during the phase of stable crack growth the crack propagation rate is higher then under constant amplitude loading until approximately 9 MPa $m^{1/2}$.

As reported for single overloads in the analysed alloy [3,4] the observed crack growth trends for periodic overloads are consistent with the plasticity-induced closure phenomenon. Each overload produces higher monotonic plastic zone than the baseline loading. As the crack grows into the compressive residual stress field formed by the overload cycle it encounters increased levels of plasticity that induce near tip closure. This results in an increase of the crack opening load which implies a reduction of the minimum effective driving force behind the crack. The corresponding crack growth rates must therefore be lower as indeed observed.

The retardation effect is more pronounced when overloads were applied at a periodicity near the number of cycles at which the minimum value of the crack growth rate for the equivalent single overload was reached. When the overload is applied still in the period when crack growth rates are decreasing it suspends the crack delay due to the previous overload, reducing this way the retardation effect.

The apparent contradiction observed for n_{BL}=10, *i.e.*, simultaneous higher crack closure and crack growth rates than in constant amplitude loading, is not necessarily in disagreement with the plasticity-induced closure argument because too closely spaced overloads lead to acceleration rather than retardation since crack jump at each overload greatly exceeds the retardation in the subsequent few baseline cycles.

3.4. Prediction from crack closure measurements

The crack growth rates inferred directly from the experimental closure measurements depicted in Fig. 4 and the characteristic *da/dN* versus DK_{eff} relation of the material are compared with the experimental crack growth rates in Fig. 5. The characteristic *da/dN* versus DK_{eff} relation of the material, which was determined in previous work [3], is given by Eq. (4):

$$\frac{da}{dN} = 1.23\times10^{-7}\left(\Delta K_{eff}\right)^{3.39} \qquad 2.5\leq\Delta K_{eff}\leq 12 \qquad (4)$$

where *da/dN* and DK_{eff} are in mm/cycle and MPa $m^{1/2}$, respectively.

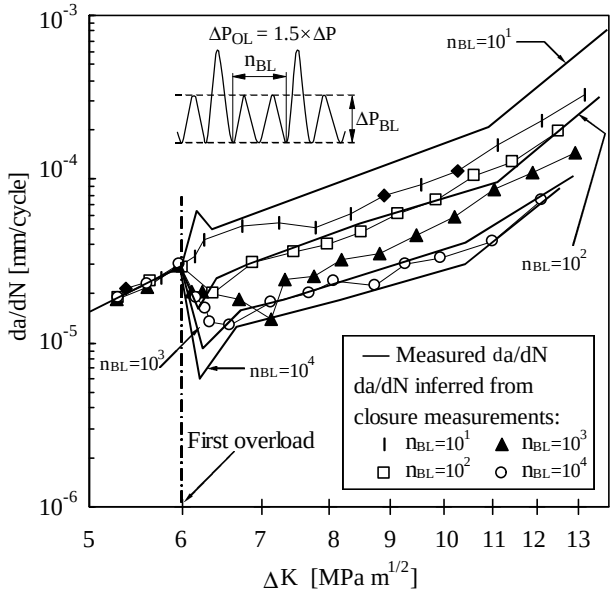

Fig. 5. Comparison between predicted from closure measurements and experimental crack growth rates.

In site of crack closure being able to correlate the majority of the crack growth transients and also the periodicity effect, the inferred and measured crack growth rates show good agreement only for the load sequence containing overloads applied with 100 intermediate baseline cycles. For closely spaced overloads (n_{BL}=10) the predicted crack growth rates are lower and for n_{BL}=1 000 and n_{BL}=10 000 higher than experimental ones.

As already mentioned, the crack closure levels presented in Fig. 4 are mean values. Therefore, the discrepancy between inferred and experimental crack growth rates reinforces the idea that closure based damage models must perform a cycle by cycle analysis in order to achieve warrantable predictions.

3.5. Analysis of fatigue fracture surfaces

Fig. 6 shows the typical features of the fatigued fracture surfaces. The images presented were obtained close to the centre of the specimens. The crack growth direction is from bottom do top in all figures.

Fig. 6(a) (ΔK=7.5MPa $m^{1/2}$, da/dN=1.4×10^{-5}mm/cycle) corresponds to the stable crack growth rate stage following the first overload. This figure shows a marking line after each overload cycle similar to that

observed following single peak overloads [4]. As expected, the spacing between these markings increases with crack length because the crack growth rate increases with *DK*.

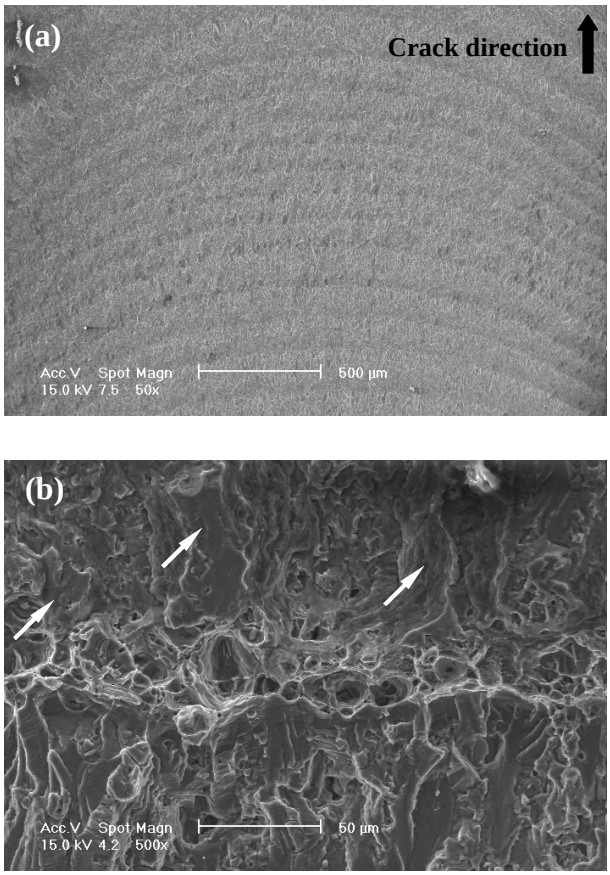

Fig. 6. SEM images of fatigued fracture surfaces, R=0.05 and n_{BL}=10 000: (a) marking lines, (b) effect of the overload cycle at high *DK* values.

Fig. 6(b) (ΔK=12.5MPa $m^{1/2}$,da/dN=8.1×10^{-5}mm/cycle) shows an intense formation of dimples at high *DK* values due to the strong plastic deformation during the overload cycle. Typical fatigue fracture surfaces of AlMgSi1-T6 have a chaotic wavy appearance with relative rough areas [4]. However, the post-overload region exhibits intense smeared zones (marked by arrows) denoting increased contact between crack faces and, therefore, of crack closure levels.

4. CONCLUSIONS

1. For remotely spaced overloads crack retardation is observed, while the results for closely spaced overloads present crack acceleration.

2. Crack retardation increases with overload periodicity and decreases with stress ratio increase.

3. The crack closure data show basically the same trend as the corresponding experimentally observed crack growth rate response. Moreover, the influence of overload spacing is in agreement with the different closure levels.

4. In spite of some discrepancy, attributed to the quick change of the closure levels, it is clear that plasticity induced crack closure plays an important role on the load interaction effects observed in this aluminium alloy.

ACKNOWLEDGEMENTS

The authors would like to acknowledge POCTI programme, project 1999/EME/32984, for funding the work reported.

REFERENCES

[1] Shin, C.S., and Hsu, S.H., "On the mechanisms and behaviour of overload retardation in AISI 304 stainless steel", Int. J. Fatigue, 15, 181-192 (1993).

[2] Shuter, D.M. and Geary, W., "The influence of specimen thickness on fatigue crack growth retardation following an overload", Int. J. Fatigue, 17, 111-119 (1995).

[3] Borrego, L.P., Ferreira, J.M. and Costa, J.M., "Fatigue crack growth and crack closure in an AlMgSi alloy", Fatigue Fract. Engng Mater. Struct., 24, 255-265 (2001).

[4] Borrego L.P., Ferreira J.M., Pinho da Cruz J.M and Costa J.M. "Evaluation of overload effects on fatigue crack growth and closure", Engng Fract. Mech., 70, 1379-1397 (2003).

[5] Vardar, O., Yildirim, N., "Crack growth retardation due to intermittent overloads", Int. J. Fatigue, 12, 283-287 (1990).

[6] Ohrloff, N., Gysler, A., Lütjering, G., "Fatigue crack propagation behaviour under variable amplitude loading", in: Fatigue Crack Growth Under Variable Amplitude Loading (Ed. Petit J., Davidson D.L., Suresh S., Rabbe P.), Elsevier, 24-34. (1988).

[7] American Society for Testing and Materials, "Standard test method for measurements of fatigue crack growth rates", Annual Book of ASTM Standards: Volume 03.01, ASTM E 647, 562-598 (1995).